

Rhodopsin Photoproducts in 2D Crystals

Reiner Vogel^{1*†}, Jonathan Ruprecht^{2†}, Claudio Villa², Thorsten Mielke²
Gebhard F. X. Schertler² and Friedrich Siebert¹

¹*Biophysics Group, Institut für Molekulare Medizin und Zellforschung
Albert-Ludwigs-Universität
Freiburg, Hermann-Herder-Str.
9, D-79104 Freiburg, Germany*

²*Structural Studies Division
MRC Laboratory of Molecular
Biology, Hills Road, Cambridge
CB2 2QH, UK*

The published electron microscope and X-ray structures of rhodopsin have made available a detailed picture of the inactive dark state of rhodopsin. Yet, the photointermediates of rhodopsin that ultimately lead to the activated receptor species still await a similar analysis. Such an analysis first requires the generation and characterization of the photoproducts that can be obtained in crystals of rhodopsin. We therefore studied with Fourier-transform infrared (FTIR) difference spectroscopy the photoproducts in 2D crystals of bovine rhodopsin in a $p22_12_1$ crystal form. The spectra obtained by cryotrapping revealed that in this crystal form the still inactive early intermediates batho, lumi, and meta I are similar to those obtained from rhodopsin in native disk membranes, although the transition from lumi to meta I is shifted to a higher temperature. However, at room temperature, the formation of the active state, meta II, is blocked in the crystalline environment. Instead, an intermediate state is formed that bears some features of meta II but lacks the specific conformational changes required for activity. Despite being unable to activate its cognate G protein, transducin, to a significant extent, this intermediate state is capable of interacting with functional transducin-derived peptides to a limited extent. Therefore, while unable to support formation of rhodopsin's active state meta II, 2D $p22_12_1$ crystals proved to be very suitable for determining 3D structures of its still inactive precursors, batho, lumi, and meta I. In future studies, FTIR spectroscopy may serve as a sensitive assay to screen crystals grown under altered conditions for potential formation of the active state, meta II.

© 2004 Elsevier Ltd. All rights reserved.

*Corresponding author

Keywords: infrared spectroscopy; protein conformation; G protein-coupled receptor; membrane protein; visual pigment

Introduction

Rhodopsin is the visual pigment responsible for dim light vision in the rod photoreceptor cells. It constitutes a prototype within class A of the large

family of G protein-coupled receptors (GPCRs) that play an important role in transmembrane signaling.^{1,2} Recently published X-ray structures from 3D crystals of bovine rhodopsin have provided us with a detailed picture of the inactive dark state of rhodopsin.^{3,4} They have confirmed the arrangement of rhodopsin's seven membrane-spanning helices proposed from homology data,⁵ and from projection structures obtained from 2D crystals of rhodopsin by means of electron cryomicroscopy.^{6–9}

From the archaeal light-driven proton pump bacteriorhodopsin, another example of a retinal-bound membrane protein with seven transmembrane helices, 3D crystals can be obtained that remain stable under continuous illumination. This facilitated the collection of diffraction data and the calculation of 3D structures from the ground state of bacteriorhodopsin and from intermediates of its photocycle.^{10,11} In contrast to

† R.V. and J.R. contributed equally to this work.

Abbreviations used: GPCR, G protein-coupled receptor; FTIR, Fourier-transform infrared; HOOP, hydrogen-out-of-plane; DMPC, dimyristoyl phosphatidylcholine; DPPC, dipalmitoyl phosphatidylcholine; DSPC, distearoyl phosphatidylcholine; POPC, palmitoyl oleyl phosphatidylcholine.

Present address: T. Mielke, Institut für Medizinische Physik und Biophysik, Charite-Universitätmedizin Berlin, Schumannstraße 20/21, D-10098 Berlin, Germany

E-mail address of the corresponding author: reiner.vogel@biophysik.uni-freiburg.de

crystals of bacteriorhodopsin, 3D crystals of rhodopsin were shown not to be stable towards illumination even at 4 °C. Instead, the crystal lattice deteriorated irreversibly after photolysis, leading to the disappearance of diffraction peaks.¹² This seriously hampers efforts to obtain a high-resolution structure of light-activated rhodopsin and to provide a detailed molecular picture of the activation mechanism, which is currently based on less direct methods.

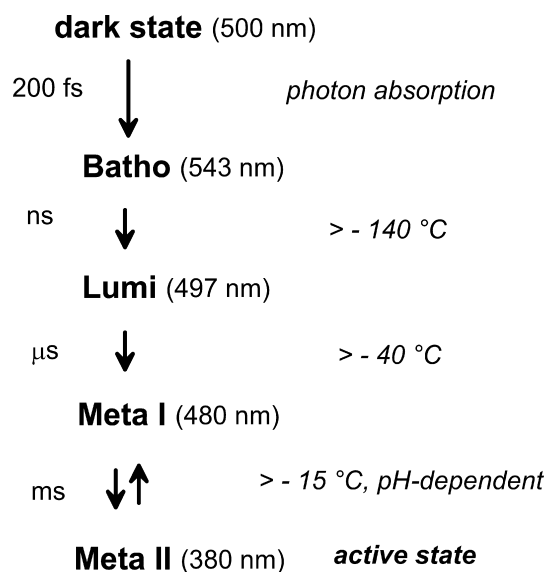
In contrast to 3D crystals, 2D crystals of rhodopsin proved to be capable of forming photointermediates even at room temperature without losing their crystalline long-range order (J.R. & G.F.X.S., unpublished results). We sought a method to characterize which photointermediates are formed in the 2D crystals, and to compare these photointermediates with those obtained in native disk membranes or in detergent solution, before initiating structural studies. The photoproducts of rhodopsin in membranes or detergent micelles have been well characterized in recent years, e.g. by means of UV-visible spectroscopy,¹³ Fourier-transform infrared (FTIR) spectroscopy,^{14,15} Raman spectroscopy¹⁶ and electron paramagnetic resonance spectroscopy of spin-labelled pigments,^{17,18} and by various biochemical assays involving the introduction of cross-links between transmembrane helices.^{19–21}

FTIR difference spectroscopy has been shown to be a particularly well suited method for sensitively monitoring the changes of both the chromophore and the protein moiety of rhodopsin in the sequence of photo intermediates.^{14,15,22} Application of this technique to 2D *p22₁2₁* crystals of rhodopsin revealed that the crystalline environment does not support the conformational changes required for the ultimate transition to the activated receptor species, meta II. Despite being able to interact with functional peptides derived from rhodopsin's cognate G protein, transducin, the room-temperature photoproduct in 2D crystals was not capable of activating transducin and thus initiating signal transduction. The transitions to the still inactive precursors of the active state were not blocked in the crystals. The difference spectra of batho, lumi, and meta I were very similar to those obtained in the native membrane environment, although the transition temperature to meta I was higher in the 2D crystals. These findings establish a basis for further structural studies on 2D crystals of rhodopsin using electron crystallography to provide us with more detailed information about the structural changes taking place in the earlier photointermediates of rhodopsin.

Results

Rhodopsin photoproducts in native disk membranes

We first give a short summary on the photoproducts of rhodopsin in its native disk membrane



Scheme 1.

environment. Illumination of the dark state of rhodopsin leads to isomerization of its covalently bound retinal chromophore from an inactivating 11-*cis* to an all-*trans* geometry. This produces in native disk membranes a series of still inactive photointermediates that can be trapped below characteristic transition temperatures (Scheme 1): batho (λ_{\max} 543 nm, $T < -140$ °C/133 K), lumi (λ_{\max} 497 nm, $T < -40$ °C/233 K), and meta I (λ_{\max} 480 nm).^{23,24} The last inactive intermediate, meta I, is in a pH and temperature-dependent equilibrium with meta II (λ_{\max} 380 nm), which can be shifted towards meta II by lowering the pH or increasing the temperature.^{25,26} Meta II represents the active receptor state, which is capable of interaction with and activation of the visual G protein, transducin. The transition to meta II involves significant conformational changes of the protein. These changes, which lead to a deprotonation of the Schiff base in meta II, render the equilibrium with its meta I precursor remarkably sensitive to pH and temperature, and to pressure, fluidity and spontaneous curvature of the lipid or detergent matrix where the protein is embedded.^{23,27–31}

Low-temperature photoproducts in 2D crystals

As a first step in the characterization of rhodopsin's photoproducts in 2D crystals, we studied the low-temperature photoproducts batho and lumi, which were stabilized by cooling the samples to -183 °C (90 K) and -93 °C (180 K), respectively, prior to photolysis, such that they could be examined by static FTIR difference spectroscopy. To characterize the different photoproduct states, we recorded spectra before and after photolysis of the sample and formed the difference between the two. In the conventional representation (photoproduct minus initial dark state), positive bands in the difference spectra belong to the photoproduct

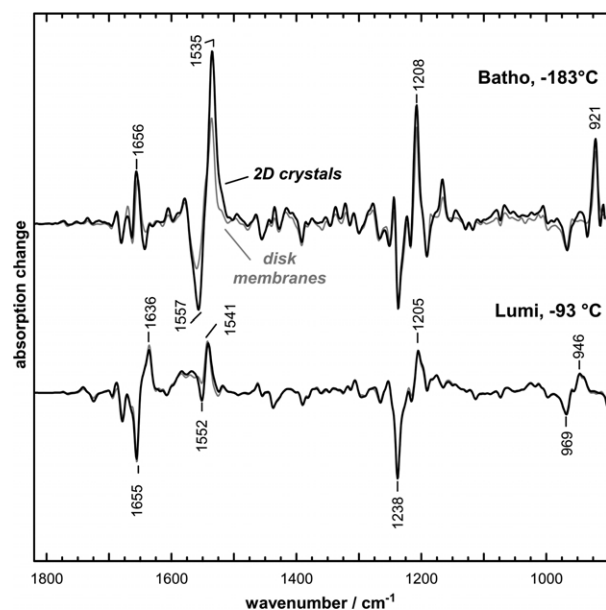


Figure 1. The transitions to the low-temperature photointermediates batho and lumi are unperturbed in 2D crystals. FTIR difference spectra were obtained at -183°C (90 K) for the batho intermediate, and at -93°C (180 K) for lumi, both from rhodopsin in 2D crystals (black) and from rhodopsin in its native disk membrane environment (grey), all at pH 7.0. In this representation (photoproduct minus dark state), vibrational bands of the initial dark state are negative, while those of the photoproduct states are positive. As the spectra obtained from 2D crystals correspond to those obtained from the membrane environment, the transitions to both batho and lumi are unperturbed by the crystalline environment.

state, while negative bands represent the initial dark state. In Figure 1, we can compare the difference spectra of batho and lumi obtained from rhodopsin in native disk membranes (grey) with the photoproducts obtained from rhodopsin in 2D crystals (black) under otherwise identical conditions. Obviously, the overall vibrational patterns of the difference spectra obtained from 2D crystals superimpose very well with those in the difference spectra obtained from disk membranes, and the vibrational marker bands of the respective states are present in both the crystalline and the membranous environment. Such markers are the strong ethylenic mode at 1535 cm^{-1} , the fingerprint mode at 1208 cm^{-1} , and the intense hydrogen-out-of-plane (HOOP) mode at 921 cm^{-1} in the case of batho, and the HOOP modes around 940 cm^{-1} , as well as the shape of the band pattern of protonated carboxylic acids above 1700 cm^{-1} and in the amide I range around 1650 cm^{-1} in the case of lumi.¹⁴ This indicates that the batho and lumi photoproduct states are regularly formed in the crystalline environment. Some slight differences are discernible in the relative amplitudes of some vibrational bands in the range around 1550 cm^{-1} of the chromophores ethylenic mode and the protein amide II modes, as well as in the fingerprint range

between 1300 cm^{-1} and 1050 cm^{-1} , reflecting the C–C stretching vibrations of the chromophore. These differences arise presumably from a higher degree of pigment orientation in samples prepared from crystals in combination with a non-vanishing linear dichroism of the involved bands, as suggested by comparison of the spectra with those obtained from membrane samples with a better orientation obtained by isopotential spin drying (F. Nüsken & F.S., unpublished results).

The batho state is stable in 2D crystals and in disk membranes below -130°C . In the temperature range between -130°C and -90°C , we found a similar temperature-dependence for the transition to lumi for the 2D crystals as compared to disk membranes.

Transition to the meta I state

In disk membranes, lumi is stable below -60°C , such that pure meta I spectra can be obtained at temperatures above -40°C . For rhodopsin in 2D crystals, stable lumi-like difference spectra can be obtained up to -30°C and pure meta I is observed only at -10°C or higher.

We studied meta I at 10°C and pH 8.5, and obtained similar difference spectra for both membranes and crystals (Figure 2A, upper spectra). Both spectra show the typical bands of the meta I photoproduct, as e.g. the positive amide I band at 1664 cm^{-1} or the HOOP difference band of the chromophore at $-969/+950\text{ cm}^{-1}$. The presence of the typical positive band at 1203 cm^{-1} of chromophore C–C stretching vibrations further indicates a protonated Schiff base in both photoproducts. Corresponding UV–visible spectra of the photoreaction obtained under the same conditions (Figure 2B) confirm a photoproduct with a protonated Schiff base with the absorption peak at 480 nm typical of meta I. For a closer examination of the protein conformation, we show in Figure 3 an enlarged view of the spectral region between 1500 cm^{-1} and 1800 cm^{-1} . As can be seen in Figure 3A, meta I difference spectra obtained from disk membranes are clearly altered at different temperatures. The bands at 1538 , 1643 , and 1664 cm^{-1} differ significantly in intensity, and the band pattern around 1700 cm^{-1} is altered. These differences are clearly not due to contributions of lumi or meta II to the meta I spectra, as contributions by their spectra (shown in shades of grey) should influence other bands as well. The identity of meta I is confirmed by the 480 nm visible absorption peak at both temperatures. Meta I spectra obtained from disk membranes therefore vary as a function of temperature, and they do so in a reproducible manner. In Figure 3B we show meta I spectra obtained from 2D crystals at 10°C and 0°C , both at pH 8.5, and again, for comparison, the meta I spectra obtained at 10°C from disk membranes. The meta I spectra obtained from the 2D crystals show a small variation with temperature and they show deviations from the spectrum

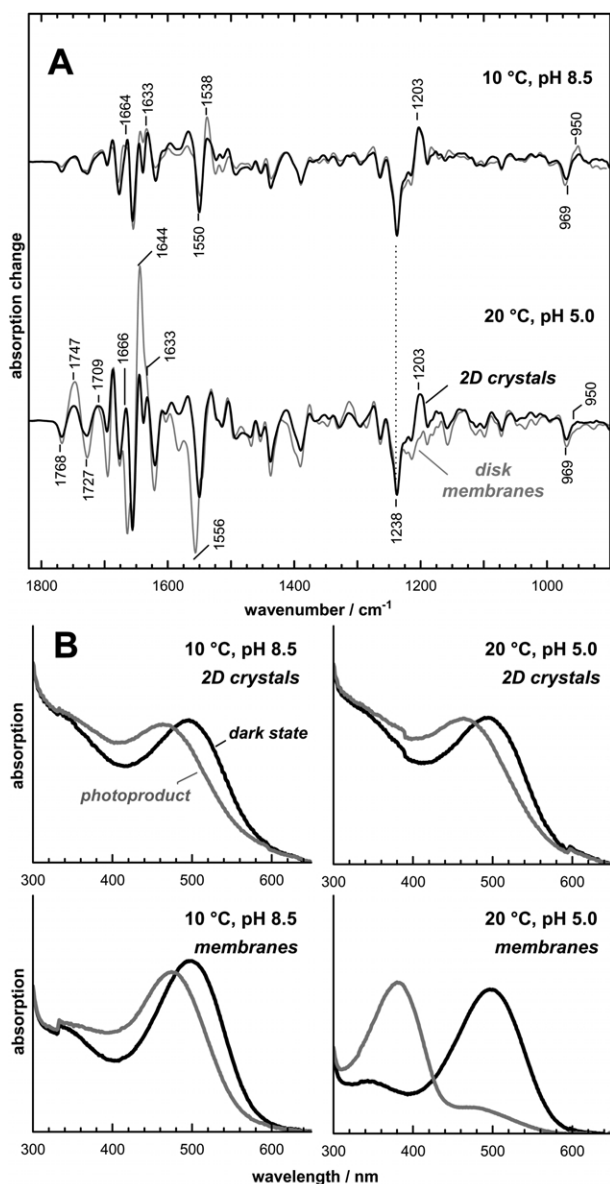


Figure 2. The transitions to the meta states. A, In native disk membranes (grey), rhodopsin forms the still inactive meta I photoproduct at 10 °C and pH 8.5, while at 20 °C and pH 5.0, the active state conformation of meta II is adopted by the protein. In 2D crystals, the meta I state corresponds to that obtained in disk membranes, while at 20 °C and pH 5.0, the transition to meta II is blocked. Instead, an intermediate state is formed with a difference spectrum that lacks some of the features of a meta II difference spectrum, as e.g. at 1747 cm^{-1} and at 1644 cm^{-1} . B, Corresponding UV-visible spectra obtained from membrane samples show the shift of the visible absorption peak from 500 nm for the dark state to 480 nm for meta I at 10 °C and pH 8.5, and to 380 nm at 20 °C and pH 5.0, reflecting the deprotonation of the retinal Schiff base in meta II. The spectra obtained from 2D crystal samples under the same conditions reveal a 480 nm photoproduct with a largely protonated Schiff base.

obtained from the disk membranes. The latter differences are particularly pronounced for the bands at 1538 cm^{-1} , 1643 cm^{-1} , and 1664 cm^{-1} . These are, however, the bands that have been

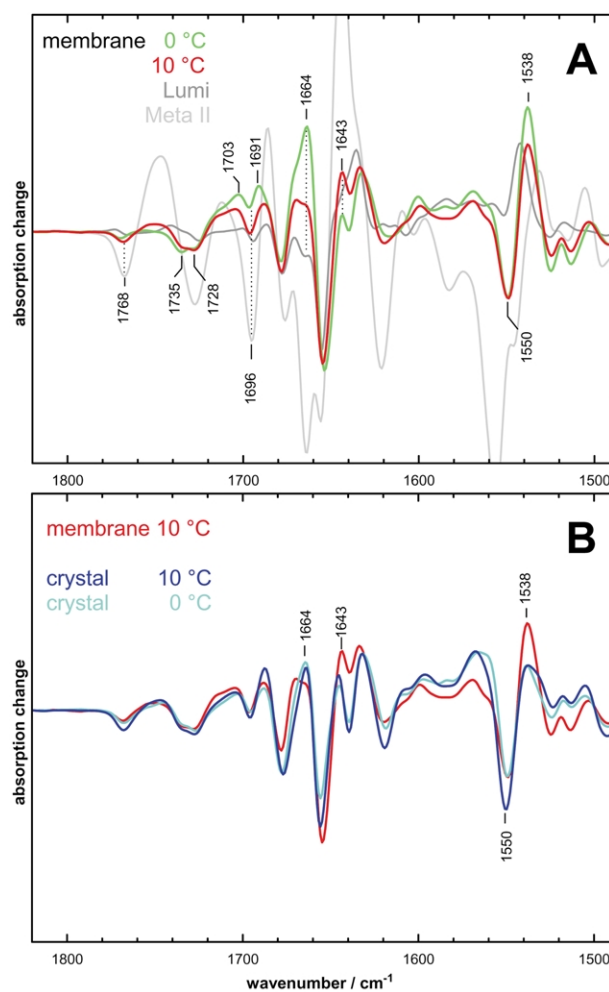


Figure 3. Comparison of the meta I states in disk membranes and in 2D crystals. A, Comparison of the 1500–1800 cm^{-1} range of meta I spectra obtained from disk membranes at 0 °C (green) and 10 °C (red), both at pH 8.5, and of lumi (dark grey) and meta II spectra (light grey) shows the intrinsic variability of meta I spectra as a function of temperature. B, Meta I spectra obtained from 2D crystals of rhodopsin at 0 °C (light blue) and 10 °C (dark blue), both at pH 8.5, do show some deviations from the meta I spectrum obtained from disk membranes at 10 °C (red). Within the naturally occurring intrinsic variability of the spectra shown in A, the spectra obtained from 2D crystals fully conform to those obtained from disk membranes.

shown to have the largest intrinsic variability in meta I in Figure 3A, and the amplitude of these differences is of comparable size. We should further keep in mind that the different degrees of pigment orientation in crystal and membrane samples may contribute to these deviations, as has been discussed above for the low-temperature states. The meta I spectra obtained from 2D crystals do therefore fully correspond to the meta I spectra obtained from disk membranes within the limits imposed by their naturally occurring intrinsic variability.

The transition to meta II is blocked in the 2D crystals

Under meta II conditions at 20 °C and pH 5.0, the photoproduct obtained in disk membranes shows the typical absorption shift to 380 nm, which reflects the deprotonation of the Schiff base in meta II (Figure 2B). In 2D crystals, on the other hand, this formation of a 380 nm photoproduct is largely absent. This is paralleled in the FTIR spectra obtained under the same conditions (Figure 2A, lower spectra). The difference spectrum obtained from disk membranes shows the typical difference bands reflecting the transition to the active state conformation of meta II. These changes involve, among others, the pronounced pattern above 1700 cm⁻¹ that arises mainly from C=O stretching vibrations of protonated carboxylic acid residues and that reflects hydrogen bonding or protonation changes of the membrane-embedded residues Asp83, Glu122, Glu113, and Glu181 (our unpublished results),³²⁻³⁴ as well as the particularly intense amide I difference band at 1644 cm⁻¹ that reflects a perturbation of the backbone structure due to the conformational transition of the protein.

For 2D crystals, the spectrum obtained at 20 °C and pH 5.0 fails to show these typical meta II marker bands. As there is no substantial deprotonation of the Schiff base in the 2D crystals, some of the deviations from the meta II spectrum obtained with disk membranes merely reflect protonation-sensitive chromophore bands, which are discussed in more detail elsewhere.³⁵ This sensitivity to Schiff base protonation explains the positive fingerprint band of the photoproduct at 1203 cm⁻¹ and the reduced intensity of the negative band at 1556 cm⁻¹, corresponding to the C=C stretching vibration of the chromophore, in the 2D crystals. The intensity of the latter band decreases considerably when the retinal Schiff base deprotonates, such that in the difference spectrum obtained from disk membranes, we see clearly the C=C vibration of the dark state, while in 2D crystals, this band is partially cancelled by the corresponding band of the photoproduct. However, other differences, particularly the reduced intensities of the positive band at 1747 cm⁻¹ corresponding to the C=O stretching vibration of protonated Asp83 and Glu122,^{32,34} and of the meta II amide band at 1644 cm⁻¹, indicate that the full conformational transition to meta II is inhibited in the 2D crystals. This is supported further by the still pronounced intensity of the slightly shifted meta I marker band at 1666 cm⁻¹. An interesting feature in the spectrum obtained from 2D crystals is the positive band centered at 1709 cm⁻¹, which is broader and less asymmetric than the corresponding band in the meta II spectrum obtained from disk membranes. In the meta II spectrum, this band is known to comprise the C=O stretching mode of Glu113, which becomes protonated in the course of receptor activation. The similar

intensities of this band in both spectra may suggest that Glu113 is protonated in the photoproduct obtained from 2D crystals, which would be in agreement with a recently proposed counterion switch occurring already during the transition to meta I.³⁶ A quantitative determination of the contribution of Glu113 to the observed band pattern in the 2D crystal photoproduct is difficult, however, due to overlapping negative bands. Furthermore, the C=O stretching vibration of protonated Glu122 absorbs in the native meta I state in the same range,³⁷ and may therefore contribute to the observed band.

Comparison to the spectrum obtained under meta I conditions (as e.g. 10 °C and pH 8.5) clearly shows that in 2D crystals, the sequence of photoproducts gets stuck in a conformation that is intermediate between that of the inactive meta I state and that of active meta II. The molecular environment of rhodopsin in the 2D crystals therefore limits the conformations accessible to the receptor compared to disk membranes.

Influence of pH, temperature, and lipid composition on the conformation of the meta states in 2D crystals

In disk membranes, the meta I/meta II equilibrium responds to a variety of parameters, e.g. temperature, pH, or the composition of its lipid environment. We therefore investigated by IR spectroscopy how far the conformation of the room-temperature intermediate state in 2D crystals responds to pH, temperature, and lipid environment, with the aim to shift it further towards that of active meta II.

As shown above, the difference spectrum obtained at 10 °C and pH 8.5 corresponds to that of meta I. Starting from these temperature and pH values, we observe the appearance of meta II marker bands (which, in the following, comprise the positive band at 1747 cm⁻¹, composed of contributions by Asp83 and Glu122, as well as the intense amide I band at 1644 cm⁻¹) upon increasing the temperature to 20 °C and/or decreasing the pH to 4.0; however, never exceeding 50% of the full intensity of these bands (as observed in disk membranes) under any of the assayed conditions. Again, the appearance of these marker bands does not imply an activation of the receptor molecule, which should be detectable by its activity towards transducin, but rather the formation of an inactive intermediate state bearing some, but not all features of meta II. Increasing the temperature to 30 °C yielded no substantial further increase of meta II features in the IR spectra (data not shown), yet decreased noticeably the stability of the photoproduct. Interestingly, we observed at 20 °C, and even more at 30 °C, a deprotonation of the retinal Schiff base in the photoproduct at alkaline pH, causing a UV-visible absorption peak at 380 nm (spectra not shown). This deprotonation, however, did not reflect formation of a

meta II state, but rather indicated a titratable Schiff base in the photoproduct, possibly due to a slightly looser protein environment of the Schiff base at these temperatures. Maybe this product corresponds to a meta I species with deprotonated Schiff base, meta I₃₈₀, which is formed transiently in disk membranes above 20 °C as shown by time-resolved UV–visible spectroscopy.³⁸

Cholesterol is known to shift the meta I/meta II equilibrium in disk membranes towards the inactive meta I state.³⁰ We therefore omitted addition of cholesterol in the crystallization protocol (see Materials and Methods) and compared the photoproducts obtained in these crystals with those from regular crystals, where cholesterol is added routinely to improve crystal quality.³⁹ However, formation of meta II was inhibited in these crystals (termed w/o cholesterol), despite the amplitude of meta II marker bands being slightly increased (compare Figure 5A). These crystals were used also in the following experiments, where we probed the interaction with G protein and G protein-derived peptides.

Activity of the room-temperature photoproduct towards G protein

We tested the capability of the room-temperature photoproduct in 2D crystals to induce nucleotide exchange and thus activation of the visual G

protein, transducin, at 20 °C at pH 5.0, pH 6.0, and pH 7.0 by a real-time fluorescence assay.⁴⁰ Unfortunately, low pH values are not accessible to G protein activation assays, as below pH 6.0, a slow spontaneous nucleotide exchange of transducin upon addition of GTP or its non-hydrolysable analog GTP γ S can be observed in the absence of pigment.⁴¹ At none of the tested pH values was a substantial activity of the photolyzed pigment in 2D crystals found, while photolyzed disk membranes activated transducin efficiently (Figure 4). In control experiments, we confirmed that the 2D crystals had the same photochemistry in the assay buffer as under our standard conditions. From the data in Figure 4, we could calculate an upper limit for the activity of the photoproduct in 2D crystals at 20 °C and pH 6.0 of 0.1% of the activity of the respective photoproduct in disk membranes, which consisted largely of meta II. At pH 5.0, due to the necessity to correct for the increased spontaneous activation of transducin and the consequent increased inaccuracy of the assay, this upper limit has to be set somewhat higher, at 2%. These results show quite clearly that the IR spectra obtained at room temperature do not reflect a meta I/meta II equilibrium with small, but detectable, pH and temperature-dependent contributions of meta II, as this would lead inevitably to a corresponding, detectable activation of transducin.

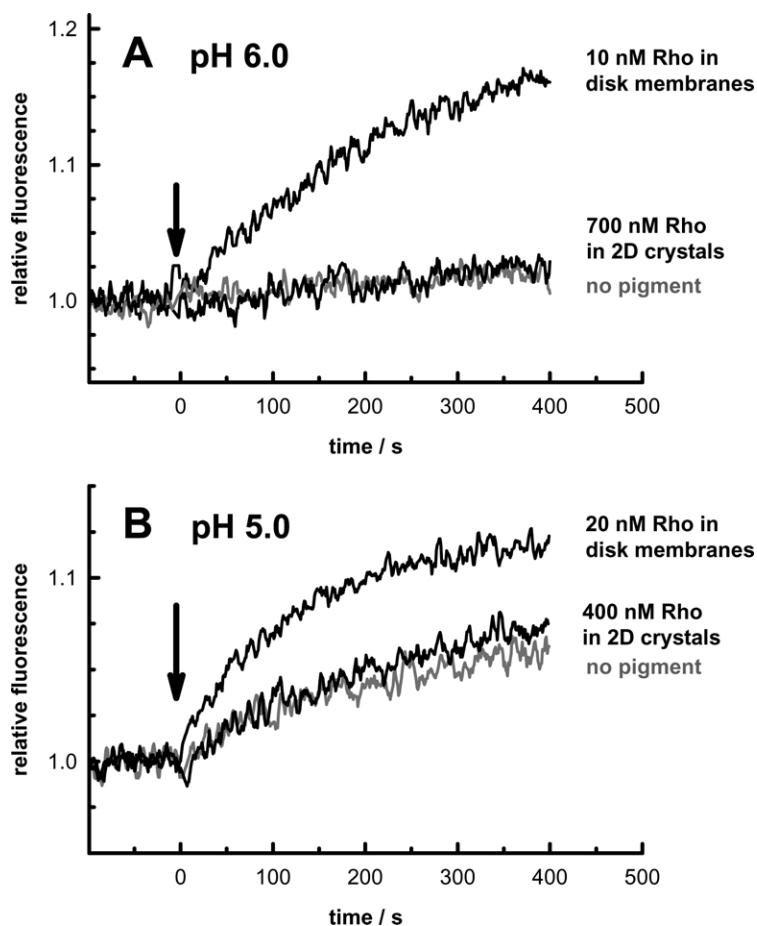


Figure 4. Rhodopsin photoproducts in 2D crystals do not activate G protein. A, Transducin activation was measured by monitoring its intrinsic fluorescence increase at 20 °C and pH 6.0 in the presence of photolyzed rhodopsin in 2D crystals (without cholesterol) or in native disk membranes. The reaction was started by adding non-hydrolysable GTP γ S, indicated by the arrow. While photolyzed rhodopsin in disk membranes activated transducin efficiently as evident from the fluorescence increase, even a 70-fold higher concentration of photolyzed rhodopsin in 2D crystals led to no higher fluorescence response compared to the control experiment without pigment, indicating an activity less than 0.1% of that of disk membranes. B, Experiments were performed as in A, but at pH 5.0, where an additional spontaneous fluorescence increase of transducin due to the lower pH is superimposed on the pigment-associated increase (see the text for details). Again, the 2D crystals show no substantial activity.

Capability of the meta photoproducts to interact with G protein-derived functional peptides

We next analyzed whether the photoproducts in 2D crystals are capable of interacting with a high-affinity analog peptide to the C terminus of the transducin α -subunit. This undecamer (acetyl-VLEDLKSCGLF) was found to bind to the active meta II intermediate in disk membranes and to shift the meta I/meta II conformational equilibrium towards meta II.⁴² The latter behavior is termed the extra-meta II effect.^{23,43,44}

In Figure 5A, we show FTIR difference spectra obtained in the presence and in the absence of peptide. By forming the difference between the two difference spectra (with peptide minus without peptide), we obtain information about conformational changes induced by the presence of the peptide. These peptide-induced double difference spectra obtained at 20 °C at pH 5.0, pH 6.0, and pH 8.5 are shown in Figure 5B.

In Figure 5C, we have calculated the corresponding peptide-induced double difference spectra for disk membranes under meta II conditions (red, 20 °C, pH 5.0) as well as under meta I conditions (blue, 10 °C, pH 8.5). The red spectrum reflects the formation of the meta II/peptide complex with characteristic positive bands at 1656 cm^{-1} , 1644 cm^{-1} , and 1535 cm^{-1} as described.^{45–47} It was found recently that the functionally similar wild-type peptide undergoes a conformational change upon complex formation with meta II,⁴⁸ such that the peptide-induced double difference spectrum obtained under meta II conditions (shown in red) likely contains the difference bands due to this conformational change.

Under meta I conditions, the presence of the peptide efficiently stabilizes the active-state conformation of meta II in disk membranes and thereby shifts the conformational equilibrium almost completely from meta I to meta II (extra-meta II effect). The corresponding peptide-induced difference spectrum (Figure 5C, blue spectrum) shows, therefore, in addition, the large difference bands due to the extra-meta II effect.

If we compare these two spectra in Figure 5C with the corresponding spectrum obtained at pH 5.0 with the 2D crystals in Figure 5B (red spectrum), it becomes evident that in the 2D crystals the key characteristics of formation of a receptor/peptide complex are there, but that there are only small contributions of the extra-meta II effect, which can be best determined from the small meta II-like difference bands visible above 1700 cm^{-1} . As all spectra are to scale (normalized by the 1238 cm^{-1} fingerprint band of dark state rhodopsin), comparison of the amplitudes of the spectra in Figure 5B with that of the red spectrum in Figure 5C allows the conclusion that, as compared to native membranes, complex formation is almost quantitative at pH 5.0, where the intermediate state is formed, but not at pH 8.5, where

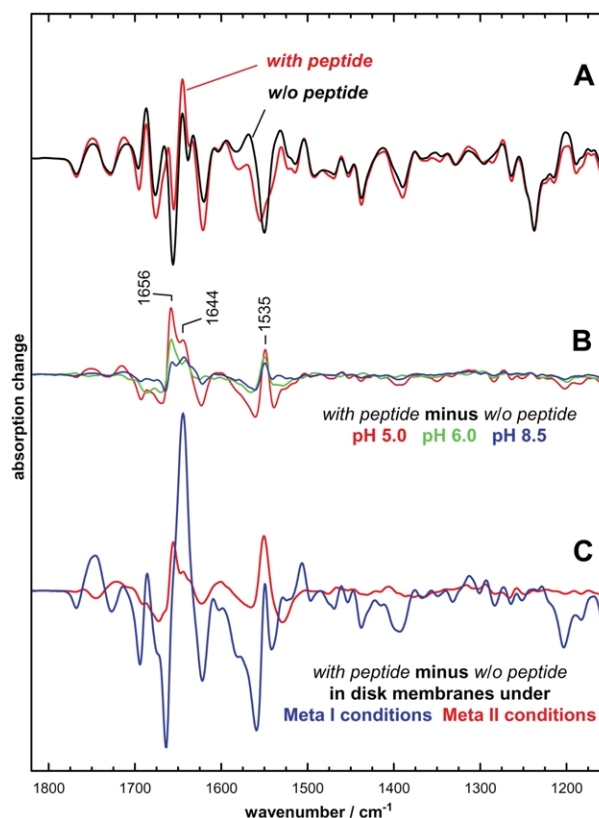


Figure 5. G protein-derived peptides interact with photoproducts in 2D crystals. A, The presence of a 20-fold excess of a high-affinity peptide analog of the transducin α -subunit C terminus gives rise to small changes in the light-induced difference spectrum obtained from rhodopsin in 2D crystals (without cholesterol) at 20 °C and pH 5.0. B, Subtraction of the spectrum obtained in the absence of peptide from that obtained in its presence yields a peptide-induced double difference spectrum, which was obtained at different pH values at 20 °C. C, Corresponding peptide-induced spectra were obtained for rhodopsin in disk membranes under meta I conditions (blue, 10 °C, pH 8.5) and meta II conditions (red, 20 °C, pH 5.0). The red spectrum, obtained under meta II conditions, shows mainly amide I and II difference bands that are evoked by structural changes within the complex that is formed quantitatively between the peptide and the active meta II photoproduct. The blue spectrum, obtained under meta I conditions, reflects in addition the peptide-induced shift of the photoproduct equilibrium of the receptor from meta I towards meta II (extra-meta II effect). A similarly pronounced extra-meta II effect can, however, not be observed in the 2D crystals. All spectra were normalized using the 1238 cm^{-1} fingerprint band of the dark state.

the conformation of the receptor corresponds rather to that of meta I. The corresponding decline of the amplitude of the peptide-induced double difference spectrum with increasing pH rules out non-specific interactions between peptide and the protein film as a source of the observed spectral changes. Therefore, despite not being able to activate transducin, the intermediate state formed at pH 5.0 is capable of interacting with the transducin-derived peptide. However, the free energy

released by formation of the receptor/peptide complex and by the structural changes induced in the peptide seems to be very small and not sufficient to induce the conformational changes required for completion of the transition to meta II.

A rigid lipid bilayer may mimic the inhibitory effect of the crystalline environment

Does the restriction of helix re-arrangement and thus the inhibition of meta II formation result from specific protein-protein contacts in the 2D crystals or are they a consequence of the increased rigidity of the crystalline environment? To tackle this question, we reconstituted purified rhodopsin in a series of saturated diacyl phosphatidylcholine lipids to study the effect of a rigid lipid environment on the conformational flexibility of the photo-receptor. The transition temperatures from the low-temperature, rigid-gel phase to the more fluid liquid-crystalline phase have been reported for aqueous dispersions of the pure lipids to be 24.0 °C for dimyristoyl phosphatidylcholine (DMPC, C₁₄), 41.5 °C for dipalmitoyl phosphatidylcholine (DPPC, C₁₆), and 54.3 °C for distearoyl phosphatidylcholine (DSPC, C₁₈).⁴⁹

At 20 °C and pH 5.0, we found in the long-chain DSPC a photoproduct with an FTIR difference spectrum very similar to those obtained from 2D crystals under same conditions (Figure 6A). Namely, the transition to meta II is blocked in DSPC. Similar results were obtained for DPPC. There, however, the amplitudes of meta II marker bands were slightly higher than in 2D crystals, but again below 50% compared to native meta II in disk membranes (not shown). In DMPC with its shorter acyl chains, the photoproduct was found to be unstable under the assayed conditions, decaying rapidly to a species bearing some of the characteristics of a non-native loose helix bundle, which has been described as a decay product of rhodopsin photoproducts in disk membranes at extreme pH.⁵⁰ In a control experiment with rhodopsin reconstituted in unsaturated palmitoyl oleyl phosphatidylcholine (POPC) or egg PC, a regular meta II spectrum was observed (not shown).

We therefore focused on DSPC and DPPC bilayers, and studied these systems in more detail. As in 2D crystals, the transition temperature between lumi and meta I was increased in both lipids. Also G protein activation and interaction with transducin-derived peptides were similar to the 2D crystals: rhodopsin reconstituted in either DSPC or DPPC bilayers was not able to activate transducin, while it showed a pronounced interaction with transducin-derived functional peptides, as shown in Figure 6B and C for the case of DSPC. Again, this interaction with the peptide was not sufficient to overcome the restraint imposed by the rigid lipid matrix onto the conformational flexibility of the protein and to induce the conformational transition to meta II. Previous

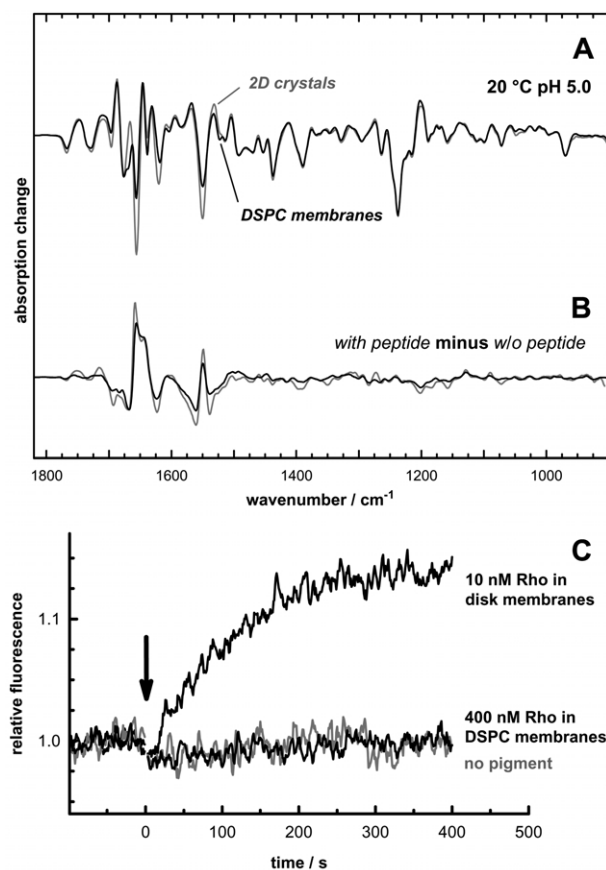


Figure 6. DSPC membrane vesicles mimic the environment of 2D crystals. A, The photoproducts of rhodopsin reconstituted into DSPC lipids (black) are very similar to those obtained from 2D crystals (grey), as shown here for the photoproduct obtained at 20 °C and pH 5.0, where the transition to meta II is blocked. B, For the interaction of the transducin α -subunit-derived peptide with this photoproduct in DSPC, characteristics similar to those of 2D crystals (see Figure 5B) were observed. Namely, the pigment is capable of interacting with the peptide, but the binding of the peptide is not sufficient to induce the conformational transition to meta II in the receptor. C, The transducin activation assay was conducted as described for Figure 4 at pH 6.0 and 20 °C. Rhodopsin in DSPC vesicles was found to be incapable of activating transducin, like rhodopsin in 2D crystals.

studies on rhodopsin reconstituted into DPPC bilayers indicated that the protein-lipid membrane partitions into rhodopsin-rich domains and rather pure lipid patches below the characteristic phase transition temperature of the recombinant membranes.⁵¹ Such a segregation of rhodopsin molecules into more densely protein-packed domains may contribute to the observed behavior in our study.

Discussion

While 3D crystals of rhodopsin are not stable under illumination even at 4 °C, but rather lose their X-ray diffraction quality,⁵² 2D crystals of

rhodopsin retain their crystalline order even when illuminated at room temperature (J.R. & G.F.X.S., unpublished results). Therefore, electron crystallography of 2D crystals seems a feasible way to obtain direct structural data of rhodopsin's room-temperature photoproducts, meta I and meta II, which form a conformational equilibrium. In contrast to the active-state meta II, its precursor meta I is not capable of activating transducin. The transition to the active state has been shown to involve a re-arrangement of the transmembrane helices, which prepares rhodopsin's cytoplasmic surface for the binding and the activation of the G protein.⁵³ This re-arrangement has been studied by a variety of means, including cross-linking of individual helices,^{20,21,54} spin-labelling,^{18,19} fluorescence decay⁵⁵ or accessibility experiments.^{56,57} Pressure relaxation techniques have further shown that this re-arrangement is accompanied by a slight expansion of the receptor molecule.^{27,28}

Our studies have shown that the conformational changes of the protein that lead to the active receptor species, meta II, are inhibited in the environment of our *p22₁2₁* 2D crystals. While a regular meta I photoproduct can be obtained at 10 °C and pH 8.5, the expected transition to meta II at lower pH and/or higher temperature is inhibited. Instead a state intermediate between meta I and meta II is formed, which has a largely protonated retinal Schiff base and is completely inactive towards rhodopsin's cognate G protein, transducin. The conformation of this intermediate state bears, to some extent, characteristics of both meta I and meta II. It shows characteristic structural marker bands of meta II, as e.g. in the frequency range of protonated carboxylic acids or in the amide I range, yet the amplitude of these bands is reduced to less than 50% of that observed in functional meta II in disk membranes. Remarkably, only the positive band at 1709 cm⁻¹ has about the same intensity as the corresponding band in meta II, although being somewhat broader and more symmetric (Figure 2A, lower spectra). Part of this positive band in the meta II difference spectra had been assigned previously to the C=O stretch vibration of Glu113, which forms the counterion to the protonated Schiff base in the dark state and becomes protonated during the transition to meta II.³³ This may indicate that protonation of Glu113, despite being a requirement for receptor activation,⁵⁸ is, in this particular case, not sufficient to pave the way to meta II.

Two properties of this intermediate state seem particularly important. First, it should not be considered as a native state of the protein, i.e. a state that reflects intrinsic properties of the protein in the disk membrane, as the known photointermediates of rhodopsin do. It rather represents an artificial state that is formed solely due to the limitations exerted by the crystalline environment on the conformational freedom of the receptor. Second, it cannot result from a merely shifted equilibrium between meta I and meta II, such that

contributions of meta II marker bands to the obtained IR difference spectrum arise from a relatively small occupancy of the meta II state under the given conditions in the 2D crystals. If this was the case, we would expect the photoproduct to be active towards transducin, to a degree corresponding to the amount of meta II that should be present to generate the observed difference spectrum. This can be clearly excluded, however, on the basis of the negative transducin activation assays. Furthermore, no substantial extra-meta II effect is observed in the presence of transducin-derived peptides in 2D crystals, despite the fact that binding of these peptides is not inhibited. Such an effect would, however, be expected in the case of a meta I/meta II conformational equilibrium.

In addition to the importance for structural studies, our results have relevance for the activation mechanism. The helix re-arrangement, which is known to be required for the transition to the active receptor species, seems to involve only a relatively small free energy gain, which is not sufficient to induce the required structural changes in the immediate environment within the crystalline matrix or to break the lattice order of the crystal. This may indicate that the expected movement of helix 6 suggested by studies performed with a variety of structurally sensitive methods (see Meng & Bourne⁵³ and references therein) should be considered as a release of interhelical constraints rather than an active pushing.

Is the inhibition of receptor activation in 2D crystals a direct consequence of the crystal lattice and the defined contacts between protein and lipid arising from it? A recent electron microscope study on the same rhodopsin *p22₁2₁* 2D crystals indicates close contacts between helices 4 and 6 of neighboring molecules,⁷ which might hint at a direct involvement of the crystalline order and of the resulting defined helix-helix contacts. On the other hand, we observe a quite identical inhibition after reconstitution of delipidated rhodopsin into the rigid environment of DSPC bilayers in the gel phase. Rhodopsin activation is known to depend on the presence of lipids with highly unsaturated fatty acid chains, which seem to form a fluid belt around the receptor molecule, as suggested by recent molecular dynamics simulations.⁵⁹ Such a solvation of the receptor is not given in a DSPC bilayer with fully saturated long acyl chains nor in the generally lipid-poor 2D crystals. The slight inhibitory effect of cholesterol in the 2D crystals further supports this notion that it is not the crystalline property of the 2D crystals alone but rather the rigidity of the immediate receptor environment, including the lipids, that prevents receptor activation. These results emphasize the importance of the interplay between protein conformational equilibria and environmental conditions.

Binding and activation of transducin to the activated receptor is known to involve at least two recognitions sites on the α and the γ -subunits of

the G protein.⁶⁰ Synthetic peptides corresponding to these recognition sites are known to interact with the receptor and to stabilize its active-state conformation.^{44,61} It was shown by FTIR spectroscopy that a large part of the induced vibrational pattern in the complex between the activated receptor and full-length transducin can be observed already in the complex with the short peptides.^{45–47} The peptide-induced changes observed in the IR difference spectra likely reflect, to some extent, conformational changes within the peptide in the complex with active meta II observed recently by transferred nuclear Overhauser effect NMR spectroscopy.^{48,62} Our observation that the low-pH, room-temperature photoproduct in 2D crystals is capable of interacting with the transducin-derived peptides, but is completely inactive towards transducin itself, is interesting and may be of more general relevance. It could suggest that the interaction of an activated receptor with its G protein consists of a sequence of at least two events: the first event involves binding and induced conformational change of at least one of the recognition sites on the G protein, giving rise to the IR signature of the receptor–peptide complex. This interaction seems to be less pronounced, if the conformation of the receptor is closer to that of meta I, yet it does not require the full structural re-arrangement of the receptor that occurs during formation of active meta II. This full helix re-arrangement is required only in the second step, which catalyzes the structural changes within the G protein, leading to nucleotide exchange in the G protein's nucleotide-binding pocket and thereby to its activation.

Our studies have revealed that the environment of rhodopsin in 2D crystals does not allow for full activation of the photoreceptor. Instead, the helix re-arrangement required for the transition to active meta II is inhibited and the sequence of photo-intermediates is blocked somewhere between meta I and meta II. Does this restriction imposed by the rigid environment also affect the earlier, inactive intermediates? Both batho and lumi, which were trapped at $-183\text{ }^{\circ}\text{C}$ and $-93\text{ }^{\circ}\text{C}$ in the 2D crystals, were very similar to their counterparts formed in native disk membranes. Also, the transition temperature between both intermediates was found not to be affected by the changed environment. Such an interference is observed only during the transition from lumi to meta I, where the transition temperature is increased in 2D crystals from $-40\text{ }^{\circ}\text{C}$ to above $-20\text{ }^{\circ}\text{C}$. This influence of the environment on the relaxation of the protein shows that the lumi to meta I transition of rhodopsin must involve small structural changes that couple to the matrix surrounding the protein. Such changes could involve slight helix deformations, which, however, should be much smaller than those involved in the activation step leading to meta II. Meta I itself does not show a unique FTIR spectrum. Instead, the intensities of meta I marker bands vary with temperature. Within the limits imposed by this intrinsic variability of meta I marker bands, the meta I spectra

obtained from the 2D crystals are very similar to those obtained from disk membranes. Therefore, irrespective of the 20–30 K upshift of the transition temperature, the resulting meta I state in 2D crystals corresponds to that observed in native disk membranes, as judged from the FTIR spectra. The inactive intermediates, which can be trapped in the 2D crystals at cryogenic temperatures in the case of batho and lumi or by lowered room temperature and/or alkaline pH in the case of meta I, seem to reflect faithfully the conformation of the respective states in native disk membranes. The 2D crystals are therefore very well suited to determine the structure of these intermediates by means of electron crystallography and to broaden our understanding of signal transduction in rhodopsin as well as other G protein-coupled receptors.

Materials and Methods

Isolation, purification, and crystallization of rhodopsin

For crystallization, rhodopsin was isolated from bovine rod outer segments, purified in lauryldimethylamine oxide by concanavalin A affinity chromatography, and crystallized according to established procedures resulting in 2D $p22_1$ crystals.⁹ To improve the yield and the quality of crystalline material, a modified protocol was used for crystallization that included the reconstitution of rhodopsin in the presence of additional cholesterol.³⁹ In some preparations, called w/o cholesterol, no exogenous cholesterol was added prior to crystallization (although there may be a small amount of endogenous cholesterol present in the 2D crystals that was not stripped off during the purification step in detergent). The 2D crystals were stored at $4\text{ }^{\circ}\text{C}$ in dialysis buffer containing 20 mM Hepes, 100 mM NaCl, 10 mM MgCl_2 , 3 mM NaN_3 , 4 mM mercaptoethanol, 4 mM DTT, 2.5% (v/v) isopropanol, adjusted to pH 7. All manipulations were performed under dim red light to avoid bleaching of the pigment.

Rhodopsin in washed disk membranes was prepared according to established procedures.⁶³ For pigment reconstitution in lipid bilayers of defined composition, rhodopsin was purified on concanavalin A in 1.2% (w/v) *n*-octyl β -D-glucoside (β -OG)⁶⁴ and mixed with the respective lipid (Sygena, Liestal, Switzerland), dissolved in 1.2% β -OG, at a molar ratio of 1:200. After short sonication and incubation for two hours on ice, this mixture (10 nmol of rhodopsin in a total volume of 100–400 μl) was dialyzed over a period of at least 36 hours against a volume of 40 ml of 1 mM phosphate buffer (pH 6.5), at $4\text{ }^{\circ}\text{C}$ in a micro-flow-through system using microdialyzer units with a 7 kDa cutoff (Pierce Biotechnology, Rockford, IL, USA) and a buffer flow-rate of 150 ml/hour. After dialysis, samples were pelleted and stored at $-80\text{ }^{\circ}\text{C}$.

FTIR spectroscopy

FTIR spectroscopy was performed with a Bruker IFS 28 spectrometer equipped with a mercury–cadmium–telluride detector. The 2D crystals were transferred from dialysis buffer to 1 mM sodium phosphate buffer (pH 6.5), by centrifugation prior to sample preparation.

We prepared sandwich samples from 0.5 nmol to 1.0 nmol of pigment in either 2D crystals, disk membranes, or defined lipid membranes as described.^{15,65} As buffers, we used 20 μ l of 200 mM sodium citrate, Mes (2-*N*-morpholinoethanesulfonic acid), or BTP (Bis-Tris-propane) buffer, in overlapping ranges, containing 200 mM NaCl. As a control, we checked that the sandwich samples of 2D crystals show the same room-temperature photochemistry in the UV-visible range as suspensions of 2D crystals.

The IR spectra were recorded in blocks of 512 scans with a spectral resolution of 4 cm^{-1} (acquisition time of one minute) and corrected for temporal baseline drifts. To initiate the photoreaction, samples were photolyzed for 30 seconds with light from a 150 W tungsten lamp fitted to fiber optics. We generally used a >530 nm long-pass filter for illumination, except for the batho and the lumi intermediates, which were obtained by illumination with light between 455 nm and 500 nm and between 435 nm and 480 nm, respectively, to allow for an efficient formation of the respective pure photoproduct.⁶⁶ Batho and lumi photointermediates were trapped at cryogenic temperatures in a custom-made, continuous-flow cryostat cooled by liquid nitrogen to the desired temperature. FTIR spectra were generally normalized using the 1238 cm^{-1} band of rhodopsin.

UV-visible spectroscopy

For UV-visible spectroscopy, sandwich samples identical with the infrared samples were used in a Perkin-Elmer Lambda 17 double-beam spectrophotometer equipped with a temperature-controlled sample holder. Illumination was similar to the IR experiments.

Transducin activation assay

Transducin was isolated from illuminated, osmotically shocked rod outer segments from bovine retinae and purified by hexylagarose chromatography essentially as described.^{67,68} Purified transducin was dialyzed against 10 mM sodium phosphate (pH 7.0), 150 mM NaCl, 2 mM MgCl_2 , 1 mM DTT, 0.1 mM phenylmethylsulfonyl fluoride, 50% (w/v) glycerol, and stored at -20°C . Transducin activation was assayed by monitoring its intrinsic tryptophan fluorescence changes upon nucleotide exchange⁴⁰ in a custom-made instrument with excitation by a deuterium lamp and a 290–310 nm band-pass filter. Fluorescence was detected in 90° geometry from a 1 ml thermostatically controlled fluorescence cuvette under continuous stirring through a >340 nm long-pass filter by a photo multiplier in single-photon counting mode. The assay was performed at 20°C in 900 μ l of 20 mM citric acid buffer (pH 5.0) or Mes (pH 6.0 and pH 7.0), 150 mM NaCl, and 2 mM MgCl_2 with 400 nM transducin and catalytic amounts of pigment. The pigment was photolyzed (>530 nm long-pass filter) and, after having recorded a fluorescence baseline for 100 seconds, nucleotide exchange was started by the addition of 50 μ l of non-hydrolysable GTP γ S to a final concentration of 10 μM . The fluorescence traces were corrected for background intensity of the system and the dilution effect and then normalized to the initial fluorescence intensity.

The relative activity was calculated from the slope of the fluorescence increase at time zero divided by that

obtained with rhodopsin in disk membranes at a given concentration of pigment. This was achieved by fitting the intensity of the fluorescence traces to the model function $I(t) = I_0 - I_\Delta \exp(-t/\tau)$ to yield the parameters I_Δ and τ . The slope at time zero was determined by forming the first derivative, yielding $d/dtI(t)|_{t=0} = I_\Delta/\tau$. In the case of a slow fluorescence response, a linear fit was used instead. In addition, the slope of the baseline prior to addition of GTP γ S was determined and accounted for by adding a corresponding linear term to the model function in the fitting procedure. This term, however, was found to be very small throughout.

FTIR experiments with transducin-derived peptides

Peptides were added in a 20-fold excess to the pigment suspensions prior to sample preparation. We used a high-affinity analog to the C terminus of the transducin α -subunit (acetyl-VLEDLKSCGLF).⁴²

Acknowledgements

We thank S. Lüdeke for helpful discussion, and B. Mayer, W. Sevenich, W. D. Schielin, P. Merkt, and K. Zander for technical assistance. Part of this work was supported by grants from the DFG (Si 278/16-3,4 to F.S. and R.V.) and Fonds der Chemischen Industrie (to F.S.), by an HFSP grant (RGP 0054/2002) and an MRC Predoctoral Fellowship (to J.R.).

References

1. Menon, S. T., Han, M. & Sakmar, T. P. (2001). Rhodopsin: structural basis of molecular physiology. *Physiol. Rev.* **81**, 1659–1688.
2. Okada, T., Ernst, O. P., Palczewski, K. & Hofmann, K. P. (2001). Activation of rhodopsin: new insights from structural and biochemical studies. *Trends Biochem. Sci.* **26**, 318–324.
3. Palczewski, K., Kumasaka, T., Hori, T., Behnke, C. A., Motoshima, H., Fox, B. A. *et al.* (2000). Crystal structure of rhodopsin: a G protein-coupled receptor. *Science*, **289**, 739–745.
4. Okada, T., Fujiyoshi, Y., Silow, M., Navarro, J., Landau, E. M. & Shichida, Y. (2002). Functional role of internal water molecules in rhodopsin revealed by X-ray crystallography. *Proc. Natl Acad. Sci. USA*, **99**, 5982–5987.
5. Baldwin, J. M. (1993). The probable arrangement of the helices in G protein-coupled receptors. *EMBO J.* **12**, 1693–1703.
6. Schertler, G. F. X., Villa, C. & Henderson, R. (1993). Projection structure of rhodopsin. *Nature*, **262**, 770–772.
7. Krebs, A., Edwards, P. C., Villa, C., Li, J. & Schertler, G. F. (2003). The three-dimensional structure of bovine rhodopsin determined by electron cryo-microscopy. *J. Biol. Chem.* **278**, 50217–50225.
8. Unger, V. M., Hargrave, P. A., Baldwin, J. M. & Schertler, G. F. X. (1997). Arrangement of rhodopsin transmembrane α -helices. *Nature*, **389**, 203–206.
9. Krebs, A., Villa, C., Edwards, P. C. & Schertler, G. F. (1998). Characterisation of an improved two-dimensional

- P22₁2₁ crystal from bovine rhodopsin. *J. Mol. Biol.* **282**, 991–1003.
10. Lanyi, J. K. & Luecke, H. (2001). Bacteriorhodopsin. *Curr. Opin. Struct. Biol.* **11**, 415–419.
 11. Kühlbrandt, W. (2000). Bacteriorhodopsin—the movie. *Nature*, **406**, 569–570.
 12. Okada, T., Le Trong, I., Fox, B. A., Behnke, C. A., Stenkamp, R. E. & Palczewski, K. X-R. (2000). X-ray diffraction analysis of three-dimensional crystals of bovine rhodopsin obtained from mixed micelles. *J. Struct. Biol.* **130**, 73–80.
 13. Lewis, J. W. & Kliger, D. S. (2000). Absorption spectroscopy in studies of visual pigments: spectral and kinetic characterization of intermediates. *Methods Enzymol.* **315**, 164–178.
 14. Siebert, F. (1995). Application of FTIR spectroscopy to the investigation of dark structures and photo-reactions of visual pigments. *Israel. J. Chem.* **35**, 309–323.
 15. Vogel, R. & Siebert, F. (2003). New insights from FTIR spectroscopy into molecular properties and activation mechanisms of the visual pigment rhodopsin. *Biospectroscopy*, **72**, 133–148.
 16. Pan, D. & Mathies, R. A. (2001). Chromophore structure in Lumirhodopsin and Metarhodopsin I by time-resolved resonance Raman microchip spectroscopy. *Biochemistry*, **40**, 7929–7936.
 17. Hubbell, W. L., Cafiso, D. S. & Altenbach, C. (2000). Identifying conformational changes with site-directed spin labeling. *Nature Struct. Biol.* **7**, 735–739.
 18. Farahbakhsh, Z. T., Hideg, K. & Hubbell, W. L. (1993). Photoactivated conformational changes in rhodopsin: a time-resolved spin label study. *Science*, **262**, 1416–1419.
 19. Farrens, D. L., Altenbach, C., Yang, K., Hubbell, W. L. & Khorana, H. G. (1996). Requirement of rigid-body motion of transmembrane helices for light activation of rhodopsin. *Science*, **274**, 768–770.
 20. Sheikh, S. P., Zvyaga, T. A., Lichtarge, O., Sakmar, T. P. & Bourne, H. R. (1996). Rhodopsin activation blocked by metal-ion-binding sites linking trans-membrane helices C and F. *Nature*, **383**, 347–350.
 21. Yu, H., Kono, M. & Oprian, D. D. (1999). State-dependent disulfide cross-linking in rhodopsin. *Biochemistry*, **38**, 12028–12032.
 22. Vogel, R. & Siebert, F. (2000). Vibrational spectroscopy as a tool for probing protein function. *Curr. Opin. Chem. Biol.* **4**, 518–523.
 23. Hofmann, K. P. (1986). Photoproducts of rhodopsin in the disc membrane. *Photobiochem. Photobiophys.* **13**, 309–327.
 24. Shichida, Y. & Imai, H. (1998). Visual pigment: G-protein-coupled receptor for light signals. *Cell. Mol. Life Sci.* **54**, 1299–1315.
 25. Matthews, R. G., Hubbard, R., Brown, P. K. & Wald, G. (1963). Tautomeric forms of metarhodopsin. *J. Gen. Physiol.* **47**, 215–240.
 26. Parkes, J. H. & Liebman, P. A. (1984). Temperature and pH dependence of the metarhodopsin I–metarhodopsin II kinetics and equilibria in bovine rod disk membrane suspensions. *Biochemistry*, **23**, 5054–5061.
 27. Lamola, A. A., Yamane, T. & Zipp, A. (1974). Effects of detergents and high pressures upon the metarhodopsin I–metarhodopsin II equilibrium. *Biochemistry*, **13**, 738–745.
 28. Attwood, P. V. & Gutfreund, H. (1980). The application of pressure relaxation to the study of the equilibrium between metarhodopsin I and II from bovine retinas. *FEBS Letters*, **119**, 323–326.
 29. König, B., Welte, W. & Hofmann, K. P. (1989). Photo-activation of rhodopsin and interaction with transducin in detergent micelles. Effect of ‘doping’ with steroid molecules. *FEBS Letters*, **257**, 163–166.
 30. Niu, S. L., Mitchell, D. C. & Litman, B. J. (2002). Manipulation of cholesterol levels in rod disk membranes by methyl-beta-cyclodextrin: effects on receptor activation. *J. Biol. Chem.* **277**, 20139–20145.
 31. Botelho, A. V., Gibson, N. J., Thurmond, R. L., Wang, Y. & Brown, M. F. (2002). Conformational energetics of rhodopsin modulated by nonlamellar-forming lipids. *Biochemistry*, **41**, 6354–6368.
 32. Fahmy, K., Jäger, F., Beck, M., Zvyaga, T. A., Sakmar, T. P. & Siebert, F. (1993). Protonation states of membrane-embedded carboxylic acid groups in rhodopsin and metarhodopsin II: a Fourier-transform infrared spectroscopy study of site-directed mutants. *Proc. Natl Acad. Sci. USA*, **90**, 10206–10210.
 33. Jäger, F., Fahmy, K., Sakmar, T. P. & Siebert, F. (1994). Identification of glutamic acid 113 as the Schiff base proton acceptor in the metarhodopsin II photo-intermediate of rhodopsin. *Biochemistry*, **33**, 10878–10882.
 34. Rath, P., DeCaluwe, L. L., Bovee-Geurts, P. H., DeGrip, W. J. & Rothschild, K. J. (1993). Fourier transform infrared difference spectroscopy of rhodopsin mutants: light activation of rhodopsin causes hydrogen-bonding change in residue aspartic acid-83 during meta II formation. *Biochemistry*, **32**, 10277–10282.
 35. Vogel, R., Fan, G. B., Siebert, F. & Sheves, M. (2001). Anions stabilize a metarhodopsin II-like photoproduct with a protonated Schiff base. *Biochemistry*, **40**, 13342–13352.
 36. Yan, E. C., Kazmi, M. A., Ganim, Z., Hou, J. M., Pan, D., Chang, B. S. *et al.* (2003). Retinal counterion switch in the photoactivation of the G protein-coupled receptor rhodopsin. *Proc. Natl Acad. Sci. USA*. In the press.
 37. Beck, M., Sakmar, T. P. & Siebert, F. (1998). Spectroscopic evidence for interaction between trans-membrane helices 3 and 5 in rhodopsin. *Biochemistry*, **37**, 7630–7639.
 38. Thorgeirsson, T. E., Lewis, J. W., Wallace-Williams, S. E. & Kliger, D. S. (1993). Effects of temperature on rhodopsin photointermediates from lumirhodopsin to metarhodopsin II. *Biochemistry*, **32**, 13861–13872.
 39. Mielke, T., Villa, C., Edwards, P. C., Schertler, G. F. & Heyn, M. P. (2002). X-ray diffraction of heavy-atom labelled two-dimensional crystals of rhodopsin identifies the position of cysteine 140 in helix 3 and cysteine 316 in helix 8. *J. Mol. Biol.* **316**, 693–709.
 40. Phillips, W. J. & Cerione, R. A. (1988). The intrinsic fluorescence of the alpha subunit of transducin. Measurement of receptor-dependent guanine nucleotide exchange. *J. Biol. Chem.* **263**, 15498–15505.
 41. Cohen, G. B., Oprian, D. D. & Robinson, P. R. (1992). Mechanism of activation and inactivation of opsin: role of Glu113 and Lys296. *Biochemistry*, **31**, 12592–12601.
 42. Martin, E. L., Rens-Domiano, S., Schatz, P. J. & Hamm, H. E. (1996). Potent peptide analogues of a G protein receptor-binding region obtained with a combinatorial library. *J. Biol. Chem.* **271**, 361–366.
 43. Emeis, D., Kühn, H., Reichert, J. & Hofmann, K. P. (1982). Complex formation between Metarhodopsin II and GTP-binding protein in bovine photoreceptor

- membranes leads to a shift of the photoproduct equilibrium. *FEBS Letters*, **143**, 29–34.
44. Hamm, H. E., Deretic, D., Arendt, A., Hargrave, P. A., König, B. & Hofmann, K. P. (1988). Site of G protein binding to rhodopsin mapped with synthetic peptides from the α subunit. *Science*, **241**, 832–835.
 45. Fahmy, K. (1998). Binding of transducin and transducin-derived peptides to rhodopsin studied by attenuated total reflection-Fourier transform infrared difference spectroscopy. *Biophys. J.* **75**, 1306–1318.
 46. Nishimura, S., Kandori, H. & Maeda, A. (1998). Interaction between photoactivated rhodopsin and the C-terminal peptide of transducin alpha-subunit studied by FTIR spectroscopy. *Biochemistry*, **37**, 15816–15824.
 47. Bartl, F. J., Ritter, E. & Hofmann, K. P. (2000). FTIR spectroscopy of complexes formed between Metarhodopsin II and C-terminal peptides from the G-protein α and γ subunits. *FEBS Letters*, **473**, 259–264.
 48. Kisselev, O. G., Kao, J., Ponder, J. W., Fann, Y. C., Gautam, N. & Marshall, G. R. (1998). Light-activated rhodopsin induces structural binding motif in G protein alpha subunit. *Proc. Natl Acad. Sci. USA*, **95**, 4270–4275.
 49. Blume, A. (1983). Apparent molar heat capacities of phospholipids in aqueous dispersion. effects of chain length and head group structure. *Biochemistry*, **22**, 5436–5442.
 50. Vogel, R. & Siebert, F. (2002). Conformation and stability of α -helical membrane proteins. 2. Influence of pH and salts on stability and unfolding of rhodopsin. *Biochemistry*, **41**, 3536–3545.
 51. Chen, Y. S. & Hubbell, W. L. (1973). Temperature- and light-dependent structural changes in rhodopsin-lipid membranes. *Expt. Eye Res.* **17**, 517–532.
 52. Okada, T. & Palczewski, K. (2001). Crystal structure of rhodopsin: implications for vision and beyond. *Curr. Opin. Struct. Biol.* **11**, 420–426.
 53. Meng, E. C. & Bourne, H. R. (2001). Receptor activation: what does the rhodopsin structure tell us? *Trends Pharmacol. Sci.* **22**, 587–593.
 54. Struthers, M., Yu, H. & Oprian, D. D. (2000). G protein-coupled receptor activation: analysis of a highly constrained, "straitjacketed" rhodopsin. *Biochemistry*, **39**, 7938–7942.
 55. Mielke, T., Alexiev, U., Glasel, M., Otto, H. & Heyn, M. P. (2002). Light-induced changes in the structure and accessibility of the cytoplasmic loops of rhodopsin in the activated MII state. *Biochemistry*, **41**, 7875–7884.
 56. Abdulaev, N. G. & Ridge, K. D. (1998). Light-induced exposure of the cytoplasmic end of transmembrane helix seven in rhodopsin. *Proc. Natl Acad. Sci. USA*, **95**, 12854–12859.
 57. Dunham, T. D. & Farrens, D. L. (1999). Conformational changes in rhodopsin. Movement of helix f detected by site-specific chemical labeling and fluorescence spectroscopy. *J. Biol. Chem.* **274**, 1683–1690.
 58. Fahmy, K., Siebert, F. & Sakmar, T. P. (1995). Photo-activated state of rhodopsin and how it can form. *Biophys. Chem.* **56**, 171–181.
 59. Feller, S. E., Gawrisch, K. & Woolf, T. B. (2003). Rhodopsin exhibits a preference for solvation by polyunsaturated docosahexaenoic acid. *J. Am. Chem. Soc.* **125**, 4434–4435.
 60. Kisselev, O. G., Meyer, C. K., Heck, M., Ernst, O. P. & Hofmann, K. P. (1999). Signal transfer from rhodopsin to the G-protein: evidence for a two-site sequential fit mechanism. *Proc. Natl Acad. Sci. USA*, **96**, 4898–4903.
 61. Kisselev, O. G., Ermolaeva, M. V. & Gautam, N. (1994). A farnesylated domain in the G protein gamma subunit is a specific determinant of receptor coupling. *J. Biol. Chem.* **269**, 21399–21402.
 62. Kisselev, O. G. & Downs, M. A. (2003). Rhodopsin controls a conformational switch on the transducin γ subunit. *Structure*, **11**, 367–373.
 63. Papermaster, D. S. (1982). Preparation of retinal rod outer segments. *Methods Enzymol.* **81**, 48–52.
 64. DeGrip, W. J. (1982). Purification of bovine rhodopsin over concanavalin A-Sepharose. *Methods Enzymol.* **81**, 197–207.
 65. Vogel, R. & Siebert, F. (2001). Conformations of the active and inactive states of opsin. *J. Biol. Chem.* **276**, 38487–38493.
 66. Ganter, U. M., Gärtner, W. & Siebert, F. (1988). Rhodopsin-lumirhodopsin phototransition of bovine rhodopsin investigated by Fourier transform infrared difference spectroscopy. *Biochemistry*, **27**, 7480–7488.
 67. Kühn, H. (1980). Light- and GTP-regulated interaction of GTPase and other proteins with bovine photoreceptor membranes. *Nature*, **283**, 587–589.
 68. Fung, B. K. K., Hurley, J. B. & Stryer, L. (1981). Flow of information in the light-triggered cyclic nucleotide cascade of vision. *Proc. Natl Acad. Sci. USA*, **78**, 152–156.

Edited by G. von Heijne

(Received 13 January 2004; received in revised form 1 March 2004; accepted 4 March 2004)